AFRL-VA-WP-TP-2002-302

IMPROVING CONTROL ALLOCATION ACCURACY FOR NONLINEAR AIRCRAFT DYNAMICS

David B. Doman
Michael W. Oppenheimer

APRIL 2002

AIR VEHICLES DIRECTORATE
AIR FORCE RESEARCH LABORATORY
AIR FORCE MATERIEL COMMAND
WRIGHT-PATTERSON AIR FORCE BASE, OH 45433-7542

REPORT DOCUMENTATION PAGE

Form Approved
OMB No. 0704-0188

1. REPORT DATE *(DD-MM-YY)*	2. REPORT TYPE	3. DATES COVERED *(From - To)*
April 2002	Conference Paper Preprint	08/01/2001 – 01/20/2002

4. TITLE AND SUBTITLE
Improving Control Allocation Accuracy for Nonlinear Aircraft Dynamics

5a. CONTRACT NUMBER
F33615-95-D-3800

5b. GRANT NUMBER

5c. PROGRAM ELEMENT NUMBER
61102F

6. AUTHOR(S)
David B. Doman (AFRL/VACA)
Michael W. Oppenheimer (Veridian Engineering)

5d. PROJECT NUMBER
2404

5e. TASK NUMBER
04

5f. WORK UNIT NUMBER
07

7. PERFORMING ORGANIZATION NAME(S) AND ADDRESS(ES)

Control Theory Optimization Branch (AFRL/VACA)
Control Sciences Division
Air Vehicles Directorate
Air Force Research Laboratory, Air Force Materiel Command
WPAFB, OH 45433-7542

Veridian Engineering
5200 Springfield Pike, Suite 200
Dayton, OH 45431-1289

8. PERFORMING ORGANIZATION REPORT NUMBER

9. SPONSORING/MONITORING AGENCY NAME(S) AND ADDRESS(ES)
AIR VEHICLES DIRECTORATE
AIR FORCE RESEARCH LABORATORY
AIR FORCE MATERIEL COMMAND
WRIGHT-PATTERSON AIR FORCE BASE, OH 45433-7542

10. SPONSORING/MONITORING AGENCY ACRONYM(S)
AFRL/VACA

11. SPONSORING/MONITORING AGENCY REPORT NUMBER(S)
AFRL-VA-WP-TP-2002-302

12. DISTRIBUTION/AVAILABILITY STATEMENT
Approved for public release; distribution is unlimited.

13. SUPPLEMENTARY NOTES
Paper to be presented at the AIAA Guidance Navigation and Control Conference, August 4 through 8, 2002.

This document was submitted to DTIC with color content. When the document was processed by DTIC, the color content was lost.

14. ABSTRACT

The forces and moments produced by a vehicle's aerodynamic control surfaces are often nonlinear functions of control surface deflection. This phenomenon limits the accuracy of state-of-the-art control allocation algorithms since all of the approaches are based on the assumption that the control variable rates are linear functions of the surface deflections and that control variable rate increments are not produced for zero deflections. The errors introduced by this assumption are currently mitigated by the robustness resulting from feedback control laws. A method for improving the performance of the feedback control/control allocation system is presented that directly attacks the inaccuracies introduced by these linear assumptions.

15. SUBJECT TERMS

16. SECURITY CLASSIFICATION OF:			17. LIMITATION OF ABSTRACT:	18. NUMBER OF PAGES	19a. NAME OF RESPONSIBLE PERSON (Monitor)
a. REPORT	b. ABSTRACT	c. THIS PAGE			David B. Doman
Unclassified	Unclassified	Unclassified	SAR	16	19b. TELEPHONE NUMBER *(Include Area Code)* (937) 255-8451

HES&S 31-15093-1

Standard Form 298 (Rev. 8-98)
Prescribed by ANSI Std. Z39-18

Improving Control Allocation Accuracy for Nonlinear Aircraft Dynamics

David B. Doman
2210 Eighth Street, Suite 21
Air Force Research Laboratory, WPAFB, OH 45433-7531
937-255-8451
David.Doman@wpafb.af.mil

Michael W. Oppenheimer
Veridian Engineering
5200 Springfield Pike Suite 200
Dayton, OH 45431-1289
937-476-2550
Michael.Oppenheimer@veridian.com

Abstract

The forces and moments produced by a vehicle's aerodynamic control surfaces are often nonlinear functions of control surface deflection. This phenomenon limits the accuracy of state-of-the-art control allocation algorithms since all of the approaches are based on the assumption that the control variable rates are linear functions of the surface deflections and that control variable rate increments are not produced for zero deflections. The errors introduced by this assumption are currently mitigated by the robustness resulting from feedback control laws. A method for improving the performance of the feedback control/control allocation system is presented that directly attacks the inaccuracies introduced by these linear assumptions. The approach is demonstrated using a dynamic inversion-based control law developed for a lifting body with four control surfaces. The commanded body rates form the input to a dynamic inversion control law that forms the inner-loop control structure. The outputs of the dynamic inversion algorithm serve as the inputs to a linear programming based control allocator. The control allocation algorithm is a mixed optimization scheme that minimizes the norm of the error and the deviation of the control input from a preferred value. Whether the underlying dynamic system is linear or nonlinear in the way that the controls affect the system state, the control allocator requires a linear approximation to the system inputs. In this work, instead of using a linear approximation to describe the control variable rate due to a control surface deflection (a control subspace, that contains the zero element), an affine relationship is utilized. This allows one to modify the input to the control allocator by providing an additional intercept term that corrects for the errors introduced by the control allocation algorithm's assumption of linearity. Since on-line control allocators perform computations at flight control system update rates, the decision about how far to move the control surface in the next time interval is critical. In order to accurately compute the next set of surface deflection commands, the local slope at the current operating point is used and the intercept is accounted for at the input to the control allocator.

1. Introduction

The forces and moments produced by aerodynamic control surfaces are often nonlinear functions of control surface deflection. This phenomenon limits the accuracy of state-of-the-art control allocation algorithms since all of the approaches are based on the assumption that the control variable rates are linear functions of the surface deflections and that the control variable rate increments are not produced for zero deflections. The errors introduced by this assumption are currently mitigated by the robustness resulting from feedback control laws. A method for improving the performance of the feedback control/control allocation system is presented that directly attacks the inaccuracies introduced by the linear assumptions.

Control allocators are used in conjunction with some type of feedback control law whose output consists of one or more pseudo-control commands. The number of pseudo-control commands is always less than or equal to the number of control effectors. Dynamic inversion control laws [1] and control allocation algorithms fit together quite naturally since the pseudo-control commands are easily identifiable.

Dynamic inversion control laws require the use of a control mixer or control effector allocation algorithm when the number of control effectors exceeds the number of controlled variables, or when actuator rate and position limits must be taken into account. It is quite common that the desired commands can be achieved in many different ways and so control allocation algorithms are used to provide unique solutions to such problems. Numerous control allocation algorithms exist and surveys of existing techniques are presented in Page, et. al. [2] and Bodson [3].

As stated previously, state-of-the-art control allocation algorithms all use the assumption that a linear relationship exists between the pseudo-control-commands ($\mathbf{d}_{des}$) and the control effector displacements ($\boldsymbol{\delta}$), i.e.,

$$\mathbf{d}_{des} = \mathbf{B}\boldsymbol{\delta} . \tag{1}$$

In the one-dimensional case, this is equivalent to a linear subspace containing the zero element, in the $\boldsymbol{\delta}, \mathbf{d}_{des}$ plane. In reality, the pseudo-controls are nonlinear functions of the surface deflections as well as other parameters $\mathbf{P}$ that typically include angle-of-attack, sideslip, and Mach number and can be represented by

$$\mathbf{d}_{des} = \mathbf{g}(\mathbf{P}, \boldsymbol{\delta}) . \tag{2}$$

At any given deflection, one could find a $\mathbf{B}$ for which $\mathbf{B}\boldsymbol{\delta} = \mathbf{g}(\mathbf{P}, \boldsymbol{\delta})$; however, the individual control effectiveness parameters (slopes) would be inaccurate.

In the one-dimensional case, Equation (1) is the equation of a line passing through the origin. Figure 1 shows a plot of a typical moment generated by a control surface as a function of control surface deflection, as well as the local and global slopes (b_{actual} and b_1, respectively) at the current operation point δ_1. As shown in Figure 1, for the one-dimensional case, Equation (1) utilizes a global slope approximation; slope b_1 is used as an entry in the $\mathbf{B}$ matrix, while the true slope is b_{actual}. In order to enforce the condition $\mathbf{B}\boldsymbol{\delta} = \mathbf{g}(\mathbf{P}, \boldsymbol{\delta})$, one must purposely introduce an error in the local slope, from b_{actual} to b_1. This error is what provides the zero element in the linear subspace. In Figure 1, P in $G_\delta(P,\delta)$ is set to P_o to indicate that a particular operating point has been established.

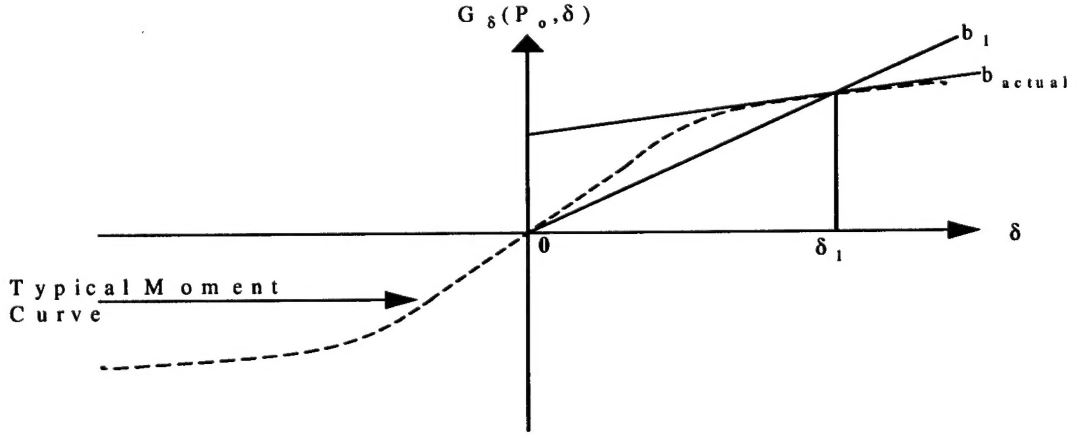

Figure 1. Error in Global Slope Approximation.

On-line control allocators must produce control effector commands at the flight control system update rate; therefore, the decision about how far to move the control surface in the next time interval is critical. In order to more accurately compute the set of surface deflection commands at the next time instant, the local slope at the current operating point can be used and the error introduced by using the local slope in the $\mathbf{B}$ matrix can be corrected by using an intercept ($\boldsymbol{\varepsilon}(\boldsymbol{\delta})$) to adjust the pseudo-control commands. In other words, we make use of an approximation for $\mathbf{g}(\mathbf{P}, \boldsymbol{\delta})$ of the form:

$$\mathbf{d}_{des} = \mathbf{g}(\mathbf{P}, \boldsymbol{\delta}) = \mathbf{B}\boldsymbol{\delta} + \boldsymbol{\varepsilon}(\boldsymbol{\delta}). \tag{3}$$

We now form a new pseudo-control command $\mathbf{d}'_{des}$ such that

$$\mathbf{d}'_{des} = \mathbf{d}_{des} - \boldsymbol{\varepsilon}(\boldsymbol{\delta}) = \mathbf{B}\boldsymbol{\delta} \ . \tag{4}$$

In a discrete-time implementation, one would use the following:

$$\mathbf{d}'_{k\,des} = \mathbf{d}_{k\,des} - \boldsymbol{\varepsilon}(\boldsymbol{\delta}_k) = \mathbf{B}_k \boldsymbol{\delta}_{k+1} \tag{5}$$

where k indicates the k^{th} time instant. At this point, any of the current linear control allocation approaches can be used to approximate the exact solution, Equation (2), with greater accuracy. In this work, we show that utilizing an affine relationship between the pseudo-control-commands and the control effector displacements can yield improvements to the control system's performance.

Using the one-dimensional case as an example, Equation (3) is equivalent to an affine subspace, that is, one, which does not contain the zero element. Stated in another fashion, $\boldsymbol{\varepsilon}(\boldsymbol{\delta})$ represents the "y-intercept" term of a line in a plane. For visualization purposes, consider a vehicle with one control surface and one axis to control. Figure 2 shows the effect of including the "intercept" term in the approximation to the control inputs. Contrary to the situation described in Figure 1, in this case, the zero element is not required. Hence, local slopes with non-zero $G_\delta(P_o,\delta)$ intercepts are acceptable. The parameters b_1 and b_2 represent the slopes of the lines that are tangent to the moment curve at δ_1 and δ_2, respectively. In other words, these slopes are the local control derivatives.

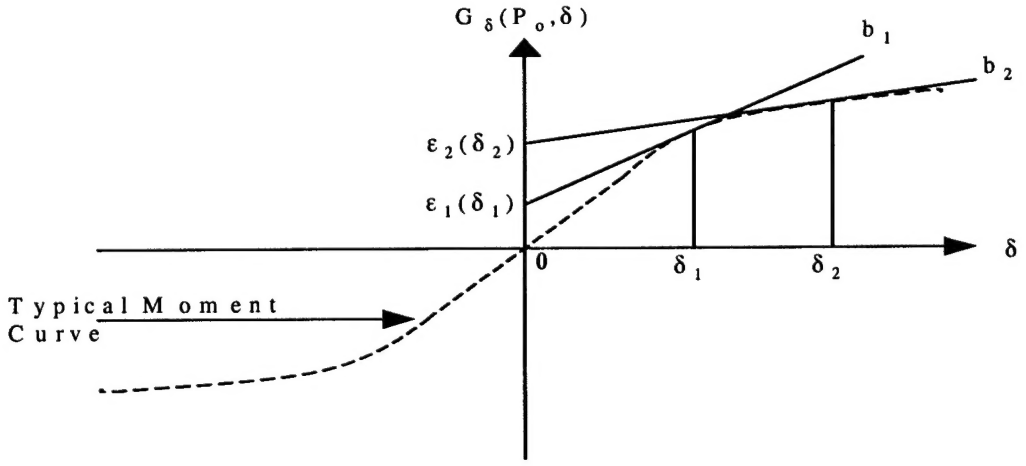

Figure 2. One-Dimensional Representation of a Moment Curve.

Figure 3 shows the impact of $\varepsilon(\delta)$ on the moments. If the control surface is operating at δ_1 without $\varepsilon_1(\delta_1)$, then the selected moment is $G_\delta(P_o,\delta_1)$ (see dashed lines). However, the selected moment should be $G_\delta(P_o,\delta_1) + \varepsilon_1(\delta_1)$. Hence, with the additional affine term included, more accurate moments are generated.

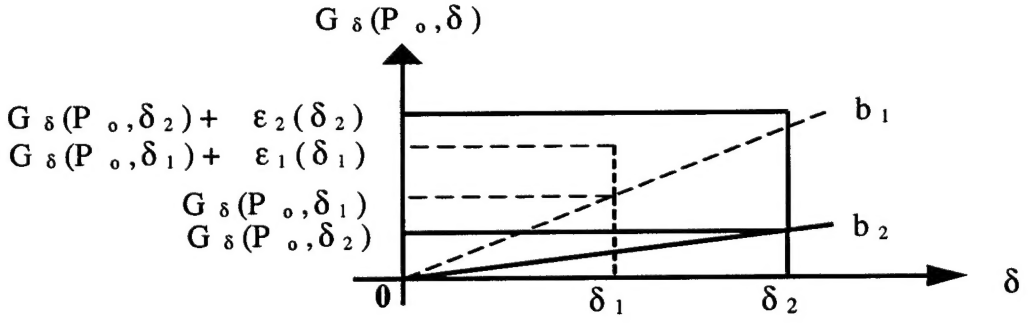

Figure 3. Effect of $\varepsilon(\delta)$ on Moment Selection.

In either of the cases discussed above, Equations (1) and (3), the moments generated by the vehicle are set equal to either a purely linear term or an affine term. Typically, a nonlinear relationship exists between these quantities; however, this nonlinear relationship cannot be solved with any control allocation algorithm, which makes the assumption that the controls can be represented by a linear or affine term. The best one can do is to reduce the errors in the approximation, hence the inclusion of $\varepsilon(\delta)$. The nonlinear behavior is a direct consequence of the model, in particular, how the inputs affect the states.

One last point that should be made is the case where the moment curve is not a monotonically increasing or decreasing function of δ. Assume, for example, that the moment curve is as shown in Figure 4. This control surface has the unusual feature that, for $\delta > \delta_p$ (the control surface location where the peak moment is produced), the moment generated is less than the moment produced at $\delta = \delta_p$.

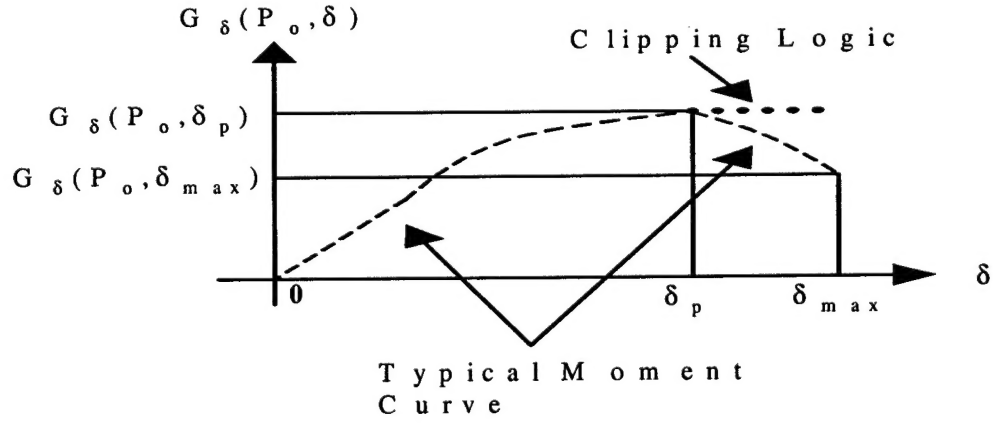

Figure 4. Non-Monotonic Moment Curve.

If the control surface is operating in the region where $\delta > \delta_p$, then, when a smaller moment is desired, instead of reducing the actuator's position towards zero, the control allocation algorithm may actually increase the actuator's position, that is, farther to the right of δ_p. In a local sense, this may be acceptable behavior, but due to actuator position limits, there is a point at which $\delta = \delta_{max}$. The control allocation algorithm will work correctly as long as the desired moment is between $G_\delta(P_o,\delta_{max})$ and $G_\delta(P_o,\delta_p)$. If a moment smaller than $G_\delta(P_o,\delta_{max})$ is requested, then the actuator position should be in a region where $\delta < \delta_p$. However, the algorithm may not move over the peak in the moment curve, effectively, limiting the

actuator's position to $\delta_p < \delta < \delta_{max}$. This is similar to the local minimum problems that occur in numerical methods. Intuitively, what should occur in this situation is the allocation algorithm should move over the "hump" in the moment curve to the region where $\delta < \delta_p$. Fortunately, this type of actuator behavior is not extremely prevalent in flight control, however, if it does occur, care must be taken to ensure proper results from the control allocation algorithm. Two solutions to this problem are as follows: force the moment curve to a monotonic function of δ using clipping logic (see dotted line in Figure 4) or reduce the position limits on δ to a point where the adverse sections of the moment curves are not available ($\delta < \delta_p$). One should notice that altering the position limit of the control surface may be undesirable because the adverse section of the moment curve for one axis may be beneficial to another axis. Likewise, clipping the moment curve results in inaccuracies in the control allocation. Hence, one must carefully balance the trade-off between the two options.

Although the theory described in this section was demonstrated using one-dimensional surfaces, this approach is directly applicable to higher-order dimension problems. If two-dimensional (two desired moments) are considered, then the moment curves in the previous figures become moment surfaces, which are functions of two independent variables.

2. Model Development and Dynamic Inversion

For the purpose of demonstration, we develop a dynamic inversion control law for a lifting-body reentry vehicle with four control surfaces. The control surfaces include two flaperons and two ruddervators.

An outer-loop control system generates body-axes angular velocity commands (p_{des}, q_{des}, r_{des}), that the inner-loop attempts to track, with the use of a dynamic inversion control law. The development of the vehicle model follows the work of Doman, et. al. [4]. The rotational dynamics of a lifting body can be written as:

$$\dot{\boldsymbol{\omega}} = \mathbf{f}(\boldsymbol{\omega},\mathbf{P}) + \mathbf{g}(\mathbf{P},\boldsymbol{\delta}) \tag{6}$$

where $\boldsymbol{\omega}$ = [p q r] and $\mathbf{P}$ denotes measurable or estimable quantities that influence the body-axes states. The parameter $\mathbf{P}$ includes variables such as angle of attack, sideslip, Mach number, and vehicle mass properties. The term $\mathbf{g}(\mathbf{P},\boldsymbol{\delta})$, in Equation (6), includes the control dependent accelerations, while the term $\mathbf{f}(\boldsymbol{\omega},\mathbf{P})$ defines accelerations that are due to the base-vehicle's aerodynamic properties. The moment equations for a lifting body in body axes [5] can be manipulated to form the control dependent and control independent terms in Equation (6). The mass properties of the vehicle under consideration are constant, thus, the time derivative of the inertia matrix can be set to: $\dot{\mathbf{I}} = \mathbf{0}$. Equation (6) becomes:

$$\dot{\boldsymbol{\omega}} = \mathbf{I}^{-1}(\mathbf{G}_B - \boldsymbol{\omega} \times \mathbf{I}\boldsymbol{\omega}) \tag{7}$$

where

$$\mathbf{G}_B = \mathbf{G}_{BAE}(\boldsymbol{\omega},\mathbf{P}) + \mathbf{G}_{\delta}(\mathbf{P},\boldsymbol{\delta}) = \begin{bmatrix} L \\ M \\ N \end{bmatrix}_{BAE} + \begin{bmatrix} L \\ M \\ N \end{bmatrix}_{\delta}, \tag{8}$$

$\mathbf{I}$ is the inertia matrix, and L, M, and N are the rolling, pitching, and yawing moments. In Equation (8), $\mathbf{G}_{BAE}(\boldsymbol{\omega},\mathbf{P})$ is the moment generated by the base aerodynamic system and $\mathbf{G}_{\delta}(\mathbf{P},\boldsymbol{\delta})$ is the sum of moments produced by the control effectors. Therefore,

$$\mathbf{f}(\boldsymbol{\omega},\mathbf{P}) = \mathbf{I}^{-1}[\mathbf{G}_{BAE}(\boldsymbol{\omega},\mathbf{P}) - \boldsymbol{\omega} \times \mathbf{I}\boldsymbol{\omega}] \tag{9}$$

and

$$\mathbf{g}(\mathbf{P},\delta)=\mathbf{I}^{-1}\mathbf{G}_{\delta}(\mathbf{P},\delta). \tag{10}$$

In order to utilize a linear control allocator, it is necessary that the control dependent portion of the model be linear in the controls. Hence, a linear approximation is developed such that:

$$\mathbf{G}_{\delta}(\mathbf{P},\delta)=\mathbf{G}_{\delta}(\mathbf{P})\delta+\varepsilon(\mathbf{P},\delta). \tag{11}$$

Using eq. (3), the model used for the design of the dynamic inversion control law becomes

$$\dot{\omega}=\mathbf{f}(\omega,\mathbf{P})+\mathbf{I}^{-1}\mathbf{G}_{\delta}(\mathbf{P})\delta+\mathbf{I}^{-1}\varepsilon(\mathbf{P},\delta). \tag{12}$$

The objective is to find a control law, which provides direct control over $\dot{\omega}$, so that $\dot{\omega}=\dot{\omega}_{des}$. Hence, the inverse control law must satisfy:

$$\dot{\omega}_{des}-\mathbf{f}(\omega,\mathbf{P})-\mathbf{I}^{-1}\varepsilon(\mathbf{P},\delta)=\mathbf{I}^{-1}\mathbf{G}_{\delta}(\mathbf{P})\delta. \tag{13}$$

Since there are more control effectors than controlled variables and the control effectors are restricted by position and rate limits, a control allocation algorithm is used. For the lifting body under consideration, there are three controlled variables, namely, roll, pitch, and yaw rates, while there are four control surfaces. Hence, a control allocation scheme must be used to insure that Equation (13) is satisfied. The control allocation scheme used in this work draws heavily on the work of Buffington, et. al. [6,7].

There are two branches in the control allocator, a sufficiency branch and a deficiency branch. The deficiency branch is used to test the feasibility of Equation (13), while the sufficiency branch is used to optimize a sub-objective when excess control authority is available. For convenience, let Equation (13) be represented by

$$\mathbf{d}'_{des}\equiv\dot{\omega}_{des}-\mathbf{f}(\omega,\mathbf{P})-\varepsilon(\mathbf{P},\delta)=\mathbf{I}^{-1}\mathbf{G}_{\delta}(\mathbf{P})\delta\equiv\mathbf{B}\delta. \tag{14}$$

If it is not feasible to obtain the relationship shown in Equation (14) due to control effector restraints, then the difference between the desired and actual effector-induced body-axis accelerations is minimized. A complete discussion of the two-branch control allocation scheme can be found in Buffington [6]. Equation (14) is in a form that makes the dynamic inversion more accurate since local slopes can be used to populate the **B** matrix and the errors introduced by using local slopes can be corrected by the intercept vector.

3. On-line Computation of Slopes and Intercepts

Aerodynamic tables that can be used to compute slopes and intercepts for the problem under consideration are generally large and the interpolation process can be slow. A common solution to storing these tables is to fit curves to the tables and store a set of basis functions and coefficients so that table entries can be estimated on-line. In this section we wish to point out that the slope and intercept data can be stored rather compactly using least-squares curve fits to an aerodynamic table that contains the moment increment due to an effector deflection over a range of effector independent parameters (**P**). Let $\mathbf{g}(\mathbf{P},\delta)$ denote the nonlinear effector data stored in the table and let **R** denote a set of basis functions that can be weighted and summed such that:

$$\mathbf{g}(\mathbf{P},\delta)\cong\mathbf{F}^{T}\mathbf{R}_{1}(\delta)+\mathbf{G}^{T}\mathbf{R}_{2}(\mathbf{P})+\mathbf{H}^{T}\mathbf{R}_{3}(\mathbf{P},\delta) \tag{15}$$

where **F, G** and **H** are vectors of constant coefficients. Thus, a curve fit for the elements of the control effectiveness matrix (**B**) can be obtained from:

$$\frac{\partial \mathbf{g}(\mathbf{P},\boldsymbol{\delta})}{\partial \boldsymbol{\delta}} \cong \mathbf{F}^{\mathrm{T}} \frac{\partial \mathbf{R}_1(\boldsymbol{\delta})}{\partial \boldsymbol{\delta}} + \mathbf{H}^{\mathrm{T}} \frac{\partial \mathbf{R}_3(\mathbf{P},\boldsymbol{\delta})}{\partial \boldsymbol{\delta}}. \tag{16}$$

Therefore, a curve fit for $\boldsymbol{\varepsilon}(\boldsymbol{\delta})$ is given by:

$$\boldsymbol{\varepsilon}(\boldsymbol{\delta}) \cong \mathbf{F}^{\mathrm{T}}\left[\mathbf{R}_1(\boldsymbol{\delta}) - \frac{\partial \mathbf{R}_1(\boldsymbol{\delta})}{\partial \boldsymbol{\delta}}\boldsymbol{\delta}\right] + \mathbf{G}^{\mathrm{T}}\mathbf{R}_2(\mathbf{P}) + \mathbf{H}^{\mathrm{T}}\left[\mathbf{R}_3(\mathbf{P},\boldsymbol{\delta}) - \frac{\partial \mathbf{R}_3(\mathbf{P},\boldsymbol{\delta})}{\partial \boldsymbol{\delta}}\boldsymbol{\delta}\right]. \tag{17}$$

Thus, the same coefficients that are used to store the slopes are also used to store the intercepts.

4. Results

A six degree-of-freedom simulation was constructed for a lifting body with four control surfaces. An inner-loop control system, consisting of prefilters, control allocation algorithm, and the plant, was constructed for the purpose of tracking commands in the rolling, pitching, and yawing moments. The inner-loop control structure is shown in Figure 5. An outer-loop control system was also developed to control the vehicle's flight-path angle, as shown in Figure 6. In Figures 5, the notation **CV** is used to represent command variables.

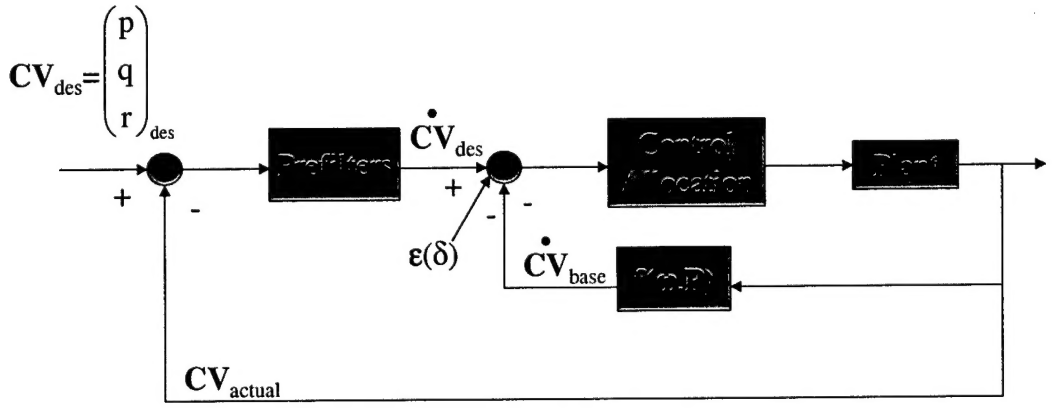

Figure 5. Inner Loop Block Diagram.

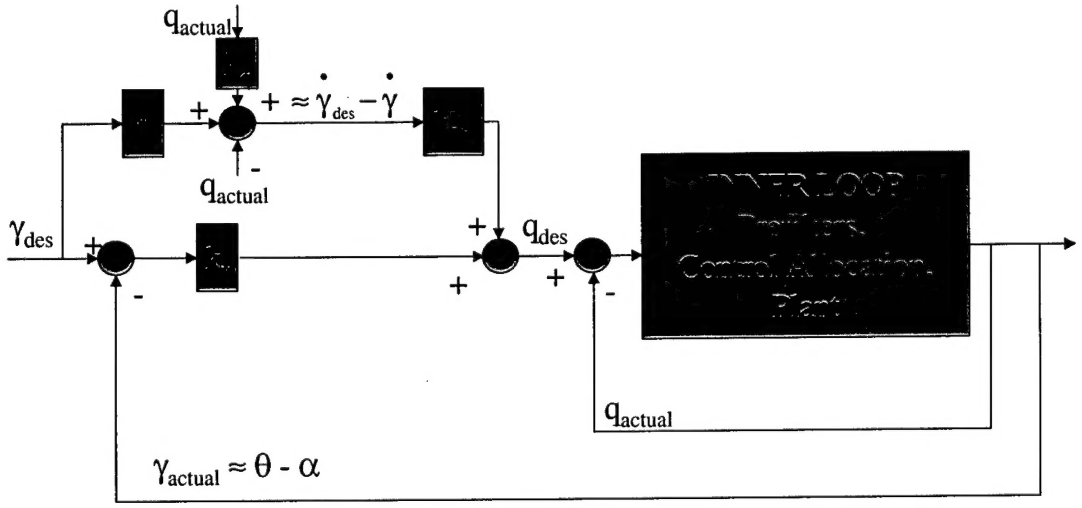

Figure 6. Flight-Path Angle Controller.

Although Figure 6 displays the proportional-derivative flight-path angle controller as only controlling the pitch axis, some other minor compensation is performed, such as, regulating sideslip.

The trajectory that was used in the simulations is as follows: the vehicle is trimmed at an initial flight-path angle of -27°. At time = 2 seconds, a -50° flight-path angle is commanded. When time = 13 seconds, the vehicle pulls up to -27° then, at time = 23 seconds, the vehicle flares to a –2.5° flight-path angle. Figure 7 shows a time history of the actual glide slopes, with and without $\varepsilon(\delta)$ compensation, and the commanded glide slope. Here, it can be determined that the actual glide slope tracks the command more accurately when $\varepsilon(\delta)$ is used.

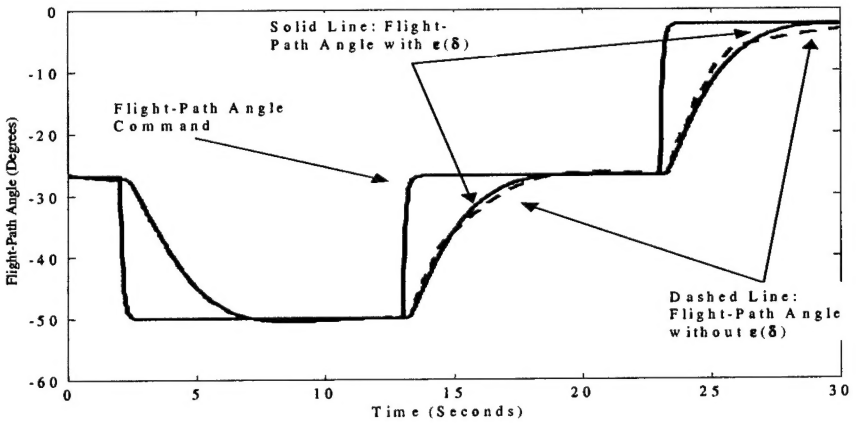

Figure 7. Flight-Path Angle Command and Responses.

In order to examine the effectiveness of the additional control allocation compensation, it is pertinent to consider the desired pitch rate and the actual pitch rate. Figure 8 shows the error in the pitch rate from the glide slope control simulation run. The two curves in Figure 8 represent the errors in pitch rate with and without $\varepsilon(\delta)$ compensation. The solid line represents the pitch rate error with $\varepsilon(\delta)$, while the dotted line shows the pitch rate error without $\varepsilon(\delta)$. It can be seen that the pitch rate errors are significantly reduced when $\varepsilon(\delta)$ is included in the control system.

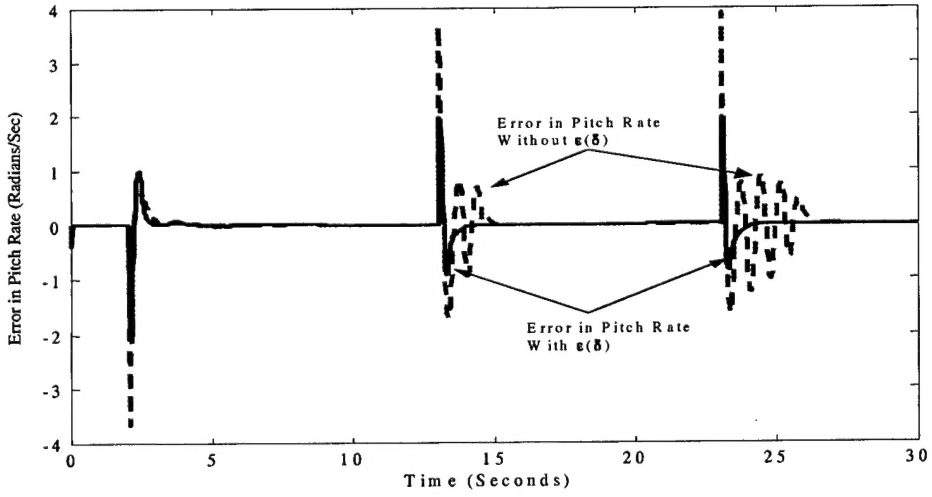

Figure 8. Error in Pitch Rates.

4. Conclusions

In a linear programming control allocation algorithm, the systems' typically nonlinear input is forced to be equal to a linear expression. Hence, fitting errors certainly affect the preciseness of the control system. To help improve the fit, an additional term was identified and added to a control allocation scheme. This term has the effect of allowing the desired set of body-axis moments to be represented by an affine subspace, instead of a linear subspace. In this way, two terms are required to represent the desired set of moments, a local slope and a corresponding "intercept" term. Some of the benefits of including this term in inner-loop control systems were also highlighted.

5. References

[1] Anon, "Application of Multivariable Control Theory to Aircraft Control Laws," Tech. Rep. WL-TR-96-3099, USAF Wright Laboratory, Wright Patterson AFB, OH, May 1996.

[2] A. B. Page and M.L. Steinberg, "A Closed-loop Comparison of Control Allocation Methods," in *Proceedings of the 2000 AIAA Guidance, Navigation, and Control Conference*, AIAA 2000-4538, Aug. 2000.

[3] M. Bodson, Evaluation of Optimization Methods for Control Allocation," in *Proceedings of the 2001 Guidance, Navigation, and Control Conference*, Aug. 2001

[4] D. Doman and A. Ngo, "Dynamic Inversion-Based Adaptive/Reconfigurable Control of the X-33 on Ascent," to appear in the *AIAA Journal of Guidance, Navigation, and Control.*

[5] B. Etkin, "Dynamics of Atmospheric Flight," John Wiley and Sons, New York 1972, pp. 143-144.

[6] J. M. Buffington, "Modular Control Law Design for the Innovative Control Effectors (ICE) Tailless Fighter Aircraft Configuration 101-3," Tech. Rep. AFRL-VA-WP-TR-1999, Air Force Research Laboratory, 1999.

[7] J. M. Buffington, P. Chandler, and M. Pachter, "Integration of On-Line System Identification and Optimization-Based Control Allocation," Tech. Rep. AIAA Paper 98-4487, American Institute of Aeronautics and Astronautics, 1998.